AFRL-RX-WP-TP-2009-4355

A MODEL FOR TRANSITIONS IN OXIDATION REGIMES OF ZrB$_2$ (POSTPRINT)

T.A. Parthasarathy, R.A. Rapp, M. Opeka, and R.J. Kerans

Ceramics Branch
Metals, Ceramics, and NDE Division

JULY 2008

AIR FORCE RESEARCH LABORATORY
MATERIALS AND MANUFACTURING DIRECTORATE
WRIGHT-PATTERSON AIR FORCE BASE, OH 45433-7750
AIR FORCE MATERIEL COMMAND
UNITED STATES AIR FORCE

NOTICE AND SIGNATURE PAGE

This report was cleared for public release by the USAF 88th Air Base Wing (88 ABW) Public Affairs Office (PAO) on 20 May 2009 and is available to the general public, including foreign nationals. Copies may be obtained from the Defense Technical Information Center (DTIC) (http://www.dtic.mil).

AFRL-RX-WP-TP-2009-4355 HAS BEEN REVIEWED AND IS APPROVED FOR PUBLICATION IN ACCORDANCE WITH THE ASSIGNED DISTRIBUTION STATEMENT.

*//Signature//

KENNETH DAVIDSON, Project Engineer
Metals Branch
Metals, Ceramics, & NDE Division
Nonmetallic Materials Division

//Signature//

MICHAEL J. KINSELLA, Chief
Ceramics Branch
Metals, Ceramics, & NDE Division

//Signature//

ROBERT MARSHALL, Asst Division Chief
Metals, Ceramics, & NDE Division
Materials and Manufacturing Directorate

*Disseminated copies will show “//Signature//” stamped or typed above the signature blocks.

REPORT DOCUMENTATION PAGE

Form Approved
OMB No. 0704-0188

1. REPORT DATE ***(DD-MM-YY)***	**2. REPORT TYPE**	**3. DATES COVERED** ***(From - To)***
July 2008	Journal Article Postprint	01 January 2007 – 01 July 2008

4. TITLE AND SUBTITLE
A MODEL FOR TRANSITIONS IN OXIDATION REGIMES OF ZrB_2 (POSTPRINT)

5a. CONTRACT NUMBER
In-house

5b. GRANT NUMBER

5c. PROGRAM ELEMENT NUMBER
62102F

6. AUTHOR(S)
T.A. Parthasarathy (UES, Inc.)
R.A. Rapp (The Ohio State University)
M. Opeka (Naval Surface Warfare Center)
R.J. Kerans (AFRL/RXLN)

5d. PROJECT NUMBER
5220

5e. TASK NUMBER
00

5f. WORK UNIT NUMBER
52200002

7. PERFORMING ORGANIZATION NAME(S) AND ADDRESS(ES)

UES, Inc.
Dayton, OH 45432

The Ohio State University
Columbus, OH

Naval Surface Warfare Center
Carderock, MD

Ceramics Branch (AFRL/RXLN)
Metals, Ceramics, and NDE Division
Materials and Manufacturing Directorate
Wright-Patterson Air Force Base, OH 45433-7750
Air Force Materiel Command, United States Air Force

8. PERFORMING ORGANIZATION REPORT NUMBER
AFRL-RX-WP-TP-2009-4355

9. SPONSORING/MONITORING AGENCY NAME(S) AND ADDRESS(ES)
Air Force Research Laboratory
Materials and Manufacturing Directorate
Wright-Patterson Air Force Base, OH 45433-7750
Air Force Materiel Command
United States Air Force

10. SPONSORING/MONITORING AGENCY ACRONYM(S)
AFRL/RXLN

11. SPONSORING/MONITORING AGENCY REPORT NUMBER(S)
AFRL-RX-WP-TP-2009-4355

12. DISTRIBUTION/AVAILABILITY STATEMENT
Approved for public release; distribution unlimited.

13. SUPPLEMENTARY NOTES
Journal article published in *Materials Science Forum*, Vols. 595-598 (2008). PAO Case Number: 88ABW-2009-2152; Clearance Date: 20 May 2009. © 2008 Trans Tech Publications. The U.S. Government is joint author of this work and has the right to use, modify, reproduce, release, perform, display, or disclose the work. Paper contains color.

14. ABSTRACT
A mechanistic model that interprets the transition in oxidation behavior of zirconium diboride as the temperature is varied from 600°C to 2500°C is presented. Available thermodynamic data and literature data for vapor pressures, oxygen permeability in boria, and viscosity of boria were used to evaluate the model. Three regimes and the temperatures of transition between them were identified. In the intermediate temperature regime, viz., 1000ºC to 1800ºC, good correspondence was obtained between theory and experiments for weight gain, recession, and scale thickness as functions of temperature and oxygen partial pressure. In this regime, the rate-limiting step is the diffusion of dissolved oxygen through a film of liquid boria in capillaries at the base of the oxidation product. At lower temperatures, an external boria scale forms, but it was not found to contribute significantly to oxidation resistance. Comparison with literature data on recession is very good, but weight gain is predicted to be higher than experimentally observed unless flow of viscous boria is included. At higher temperatures, the boria is lost by evaporation, and the oxidation rate is limited by diffusion of molecular oxygen through the capillaries between nearly columnar blocks of the oxide MO_2.; this regime is soon followed by a rapid acceleration of recession due to vaporization of the oxide MO_2 itself.

15. SUBJECT TERMS
diborides, oxidation, mechanisms, transition

16. SECURITY CLASSIFICATION OF:			**17. LIMITATION OF ABSTRACT:**	**18. NUMBER OF PAGES**	**19a. NAME OF RESPONSIBLE PERSON** (Monitor)
a. REPORT	**b. ABSTRACT**	**c. THIS PAGE**			
Unclassified	Unclassified	Unclassified	SAR	16	Kenneth E. Davidson
					19b. TELEPHONE NUMBER ***(Include Area Code)***
					N/A

Materials Science Forum Vols. 595-598 (2008) pp 823-832
online at http://www.scientific.net

A model for transitions in oxidation regimes of ZrB_2

T A Parthasarathy[1,a], R A Rapp[2,b], M Opeka[3,c], R J Kerans[4,d]

[1]UES, Inc., Dayton OH 45432

[2]The Ohio State University, Columbus, OH

[3]Naval Surface Warfare Center, Carderock, MD

[4]Air Force Research Laboratory, Materials and Manufacturing Directorate, AFRL/MLLN, Wright-Patterson AFB, OH 45433-7817

[a] Triplicane.Parthasarathy@wpafb.af.mil, [b]rapp@matsceng.ohio-state.edu,
[c]mark.opeka@navy.mil, [d]ronald.kerans@wpafb.af.mil

Keywords: diborides, oxidation, mechanisms, transition

Abstract. A mechanistic model that interprets the transition in oxidation behavior of zirconium diboride as the temperature is varied from 600°C to 2500°C is presented. Available thermodynamic data and literature data for vapor pressures, oxygen permeability in boria, and viscosity of boria were used to evaluate the model. Three regimes and the temperatures of transition between them were identified. In the intermediate temperature regime, viz., 1000ºC to 1800ºC, good correspondence was obtained between theory and experiments for weight gain, recession, and scale thickness as functions of temperature and oxygen partial pressure. In this regime, the rate-limiting step is the diffusion of dissolved oxygen through a film of liquid boria in capillaries at the base of the oxidation product. At lower temperatures, an external boria scale forms, but it was not found to contribute significantly to oxidation resistance. Comparison with literature data on recession is very good, but weight gain is predicted to be higher than experimentally observed unless flow of viscous boria is included. At higher temperatures, the boria is lost by evaporation, and the oxidation rate is limited by diffusion of molecular oxygen through the capillaries between nearly columnar blocks of the oxide MO_2.; this regime is soon followed by a rapid acceleration of recession due to vaporization of the oxide MO_2 itself.

Introduction

Diborides of refractory elements, either in pure or in composite form with SiC additions, are known to be resistant to oxidation and erosion at high temperatures [1-8]. More recent work has been prompted by the possible application in hypersonics[9-17]. However, little or no work has been reported on quantitative models of oxidation of this class of materials. A few recent works focused on thermodynamic studies[15, 18] which have identified the key solid and gaseous oxidation products. Modeling the kinetics of oxidation of this class of materials has been the focus of our research program.

In the first study, we reported on a model for the oxidation of these materials in the intermediate temperature regime, viz., ~1000C to 1800C[19]. In this report, we examine the mechanisms that operate at temperatures below 1000C, and at temperatures above 1800C. We have retained the essential elements of our prior model, but extend it to include effects that characterize the transition to the low-temperature and high-temperature regimes.

We start with a brief overview of the model for the intermediate temperature regime. Then equations are developed that describe the low and high-temperature regimes, before comparing the model to experimental data. The experimental data on these materials come from a variety of sources, whose processing methods have varied with technological advances over the past several decades. The materials have also been studied under a variety of different environmental conditions, temperature regimes and using different methods. Thus the model has to be robust to include the effects of all experimental variables to allow for a fair comparison with literature data.

Model

The key elements of the model are described in detail in [19]. Here we state, in brief, the key assumptions of the model. Fig. 1 shows a schematic of the assumed oxidation products and their morphology at steady state. The assumptions are based on reported experimental observations as noted in [19]. At low temperatures, i.e., below about 1000°C, the scale is made of columnar zirconia under an external layer of liquid boria. The boria wets the zirconia and is continuous across the zirconia scale. Oxygen diffuses through the external boria layer and then through the tortuous pathway between zirconia grains to reach the substrate. The boria and zirconia that form at the ZrB_2/ZrO_2 interface continually increase the zirconia layer thickness and the external boria thickness. The zirconia that forms is stable and is resistant to oxygen penetration due to very low ambipolar diffusion kinetics (see appendix of [19]). However, the boria either flows (viscous) or evaporates at the free surface (boundary layer diffusion limited) tending to reduce the external boria thickness. At some temperature, around 1000ºC (depending on the actual dynamic gas flow conditions), the boria evaporates so fast that the scale can no longer keep an external layer of boria. At this temperature, the oxidation transitions to an intermediate temperature regime, where the boria is still present in the scale, but only within the zirconia pores, which forms a continuous pathway. Finally, diffusion in pores is assumed to follow Fick's law, and kinetic laws are derived for planar symmetry.

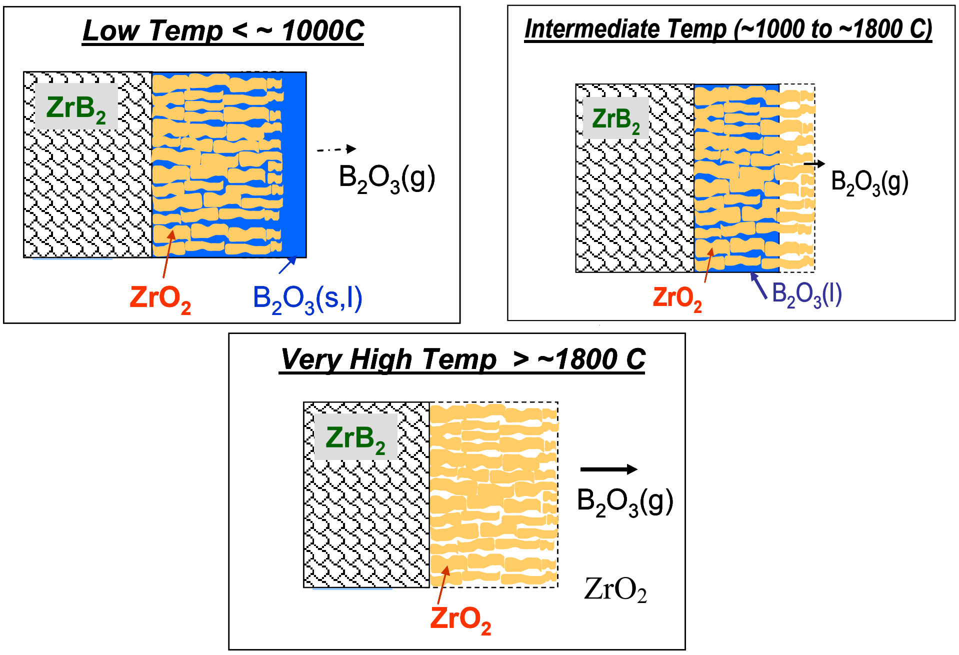

Fig. 1. Schematic sketch of the oxidation products and morphology assumed in the model.

At intermediate temperatures, the porous channels within zirconia are partially filled with boria; thus gaseous oxygen must now diffuse through part of the zirconia pore channel, and then permeate through the boria in the pore channel the rest of the way to reach the substrate. The model assumes that a quasi-steady state is reached where the amount of boria formed is balanced by the amount of boria that evaporates, which determines the depth to which the zirconia pores are filled with boria.

In this temperature regime, the ambient condition is taken to be a perfect sink for boria. The equations governing this set of mechanisms give a constant ratio of the boria thickness to zirconia thickness at any given temperature[19]. As the temperature increases, this ratio decreases until a temperature is reached where the boria evaporates and diffuses through the porous channel as fast as it is formed. Thus the mechanism evolves towards a high temperature regime. In the high temperature regime, there is no liquid boria; the scale is a dry porous zirconia. The oxidation is limited by the rate of oxygen diffusion through the porous channel. In this temperature regime, ZrO_2 also evaporates significantly, which enhances recession. The evaporation kinetics will depend on the actual dynamic flow of gases.

Model Equations

The equations describing the intermediate temperature regime can be found in Ref.[19]. Equations that relate to mass balance, gaseous diffusion, oxygen permeation rates, and thermodynamic data are the same for the low temperature and high temperature regimes and hence will not be repeated here; the reader is referred to ref. [19].

Low temperature regime. A schematic sketch of the model for low temperature oxidation kinetics is shown in Fig. 2. The length of the zirconia layer is L, and the thickness of the external boria is h_{ext}. The oxygen partial pressures are denoted by P_{O2}. We use superscripts to specify the value of parameters at the interfaces. The superscripts s, zb and a refer to the substrate/scale interface, the zirconia/boria interface, and the ambient.

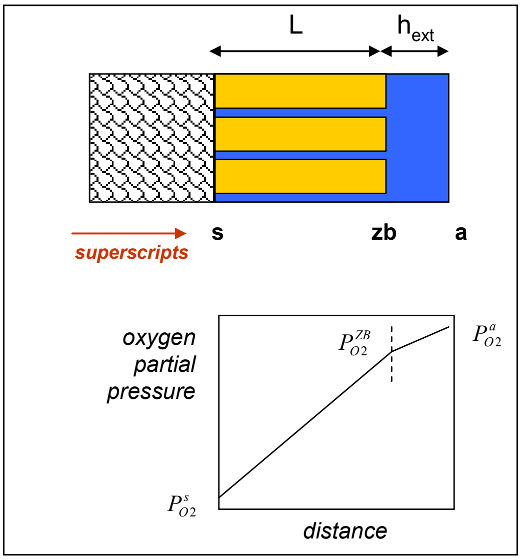

Fig. 2. A schematic sketch of the model for low temperature oxidation.

In the low temperature regime, the flux of oxygen through the external layer, must equal the flux of oxygen through the porous zirconia channel. Noting that oxygen transport occurs as permeation of molecular oxygen through liquid boria in the channels that is driven by a partial pressure gradient, the flux is given as

$$J_{O2} = f\frac{\Pi_{O2-B2O3}}{L}(P_{O2}^{ZB} - P_{O2}^{s}) = \frac{\Pi_{O2-B2O3}}{h_{ext}}(P_{O2}^{a} - P_{O2}^{ZB}) \qquad (1)$$

where J is used to denote flux, f is the fraction of pores in the zirconia, $\Pi_{O2-B2O3}$ is the permeability of oxygen in boria[20]. Rewriting equation (1), we obtain the following equations for the ratio of the layer thicknesses and the oxygen partial pressure at the zirconia/external boria interface.

$$\frac{L}{h_{ext}} = f\frac{(P_{O2}^{ZB} - P_{O2}^{s})}{(P_{O2}^{a} - P_{O2}^{ZB})} \quad or \quad P_{O2}^{ZB} = \frac{LP_{O2}^{a} + fh_{ext}P_{O2}^{s}}{fh_{ext} + L} \qquad (2)$$

Using the mass balance for the formation rates of boria and zirconia, and the inward the flux of oxygen, and combining with equation (1), we obtain the differential equation describing zirconia layer thickness growth.

$$\frac{dL}{dt} = \frac{1}{1-f}\frac{2}{5}f\frac{\Pi_{O2-B2O3}}{L}(P_{O2}^{ZB} - P_{O2}^{s})\frac{M_{ZrO2}}{\rho_{ZrO2}} \qquad (3)$$

where M and ρ refer to molecular weight and density. The rate of formation of boria as the external scale due to oxidation, $dn_{ext,B_2O_3}/dt$ (=Γ_{B2O3}) in mole per unit area per unit time, is given by the rate of formation of boria at the substrate less that which resides in the porous zirconia and that which evaporates from the surface.

$$\Gamma_{B2O3} = \frac{dn_{ext,B_2O_3}}{dt} = \left[\frac{dL}{dt}\frac{(1-f)}{(M_{ZrO_2}/\rho_{ZrO_2})} - f\frac{dL}{dt}\frac{\rho_{B_2O_3}}{M_{B_2O_3}} - J_{evap(B_2O_3)}\right] \qquad (4a)$$

$$\frac{dh_{ext}}{dt} = \Gamma_{B2O3}\frac{M_{B2O3}}{\rho_{B2O3}} \qquad (4b)$$

At low temperatures where boria is too viscous to flow, the thickness evolution of the external boria scale is given by Equation 4(b). At temperatures where the viscosity of the boria is low, significant flow of boria will occur and this will determine the external thickness, as given by the following equation.[21]

$$h_{ext} = \left[\frac{3(\Gamma_{B2O3}l_{spec})\eta_{B2O3}}{g\rho_{B2O3}^{2}\sin(\phi)}\right]^{1/3} \qquad (4c)$$

where l_{spec} is the vertical dimension of the sample, g the acceleration due to gravity, η_{B2O3} viscosity of boria (data from [22]), ϕ the angle the face subtends to the horizontal (90° for suspended specimens). The rate of evaporation of boria at the surface, under boundary-layer-limited diffusion is given by the following set of equations that include the flow velocity of the ambient gases V, its viscosity η, gaseous diffusion coefficient D, and specimen length L_{spec}.

$$J_{evap,B_2O_3} = D_{B_2O_3}\frac{(P_{B_2O_3}^{a} - P_{B_2O_3,\infty})/RT}{\delta}$$

$$\delta = function(1.5L_{spec}N_{Sc}^{-1/3}N_{Re}^{-1/2}, furnace\ size) \qquad (5)$$

$$N_{Sc} = \frac{\eta}{\rho D}; N_{Re} = \frac{\rho VL_{spec}}{\eta}$$

Following Graham and Davis [23], the effect of the boundary-layer-limited diffusion can be related to the maximum evaporation rate given by the Langmuir equation, through a parameter, α, to describe the evaporation efficiency under the actual laboratory condition.

$$\alpha = \frac{J_{evap(B2O3)}}{J_{evap(B2O3),\max}} = \frac{J_{evap(B2O3)}}{P_{B2O3}/(2\pi M_{B2O3}RT)^{0.5}} \tag{6}$$

Finally, the weight change per unit area, ΔW/A, and recession, R, are given by:

$$\frac{\Delta W}{A} = L\rho_{ZrO_2}(1-f) + (h_{ext} + fL)\rho_{B_2O_3} - R\rho_{ZrB_2} \tag{7}$$

$$R = L(1-f)\frac{M_{ZrB_2}/\rho_{ZrB_2}}{M_{ZrO_2}/\rho_{ZrO_2}} \tag{8}$$

The differential equations (3) and (4) are solved numerically, and used to predict weight change, recession, and external scale thicknesses.

High temperature regime. The high temperature regime has a much simpler structure for the scale, as shown in Fig. 3. The zirconia thickness is taken to be L, the superscripts s and a refer to the substrate and ambient. The partial pressures of boria and oxygen at the substrate/oxide interface are related through the following equation.

$$P^s_{O_2} = \left(\frac{a_{ZrO_2}}{K_{reaction}a_{ZrB_2}}\right)^{2/5}\left(P^s_{B_2O_3}\right)^{2/5} = 2.03x10^7\, exp(-\frac{81693}{T})\left(P^s_{B_2O_3}\right)^{2/5} \tag{9}$$

The flux of oxygen and boria, and the balance of fluxes give the following relationships.

$$\left|J_{O_2}\right| = \frac{5}{2}\left|J_{B_2O_3}\right|; \quad \left|J_{O_2}\right| = f\, D_{O_2}\frac{C^a_{O_2} - C^s_{O_2}}{L}; \quad J_{B_2O_3} = f\, D_{B_2O_3}\frac{C^s_{B_2O_3} - C^a_{B_2O_3}}{L}; \tag{10}$$

Combining equations (9) and (10), gives the following polynomial for oxygen concentration at the substrate, $C^s_{O_2}$.

$$D_{O_2}C^s_{O_2} + \frac{5}{2}D_{B_2O_3}\left[1.7x10^{-26}\, exp(\frac{204232}{T})\right]RT^{3/2}\left(C^s_{O_2}\right)^{5/2} = \frac{5}{2}D_{B_2O_3}C^a_{B_2O_3} + D_{O_2}C^a_{O_2} \tag{11}$$

At these high temperatures (>1800C), the vapor pressures of boria are so high that $C^a_{B_2O_3}$ =0 is a good assumption. The scale growth and recession are then given by:

$$\frac{dL}{dt} = \left(\frac{1}{1-f}\right)\left(\frac{2}{5}f\, D_{O_2}\frac{C^a_{O_2} - C^s_{O_2}}{L}\right)\frac{M_{ZrO_2}}{\rho_{ZrO_2}} - J_{evap,ZrO2} \tag{12}$$

$$\frac{dR}{dt} = \left[\left(\frac{1}{1-f}\right)\left(\frac{2}{5}f\, D_{O_2}\frac{C^a_{O_2} - C^s_{O_2}}{L}\right)\frac{M_{ZrO_2}}{\rho_{ZrO_2}}\right](1-f)\frac{M_{ZrB_2}/\rho_{ZrB_2}}{M_{ZrO_2}/\rho_{ZrO_2}} \tag{13}$$

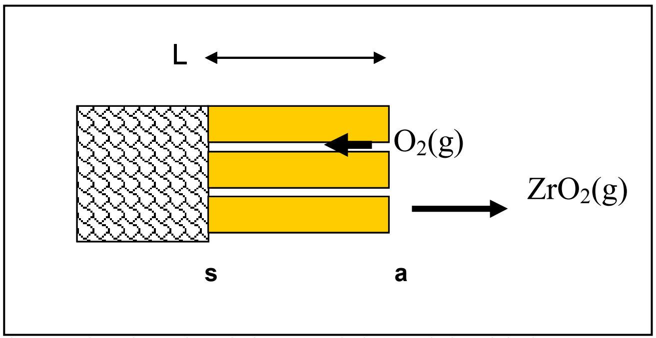

Fig. 3. A schematic sketch of the model used for high temperature regime.

The evaporation rate of zirconia at high temperatures cannot be neglected. Using thermodynamic data on vapor pressure of ZrO_2 from Barin [24] the evaporation rate under boundary-layer-limited diffusion conditions is given as:

$$J_{ZrO_2} = D_{ZrO_2}\frac{P_{ZrO_2}/(RT) - C^{\infty}_{ZrO_2}}{\delta} = \alpha\frac{P_{ZrO_2}}{2\pi M_{ZrO_2}RT};\quad P_{ZrO_2}, atm = 3x10^{10}\exp(-\frac{96369}{T}) \qquad (15)$$

Comparison of Model Predictions with Experimental Data

There are limited data in the literature on the low-temperature and high-temperature regimes of oxidation of the diborides. For the low temperature data, the weight-gain measurements of Tripp and Graham [8] conducted by TGA using 0.033 MPa of pure oxygen were considered the most appropriate data. The data of parabolic rate constant by Kuriakose and Margrave[25] at 0.099 MPa O_2 was also considered. For the high-temperature oxidation, the only data available are the recession data summarized by Fenter[7] from the work of Clougherty et al.[1, 2, 6]. Some calculated model parameters that result from the experimental conditions of quoted data are shown listed in Table 1.

Table.1 Experimental conditions and resulting model parameters at 1273K

Reference	Environment	velocity	sample length	Temp (K)	Diffusivity (B_2O_3)	δ	α
		(m/s)	(m)	(K)	(m2/s)	(m)	
Tripp,Graham	250Torr O2	0.005	0.02	1173	1.37E-04	0.0424	2.17E-05
Kuriakose, Margrave	740Torr O2	0.09	0.005	1173	7.44E-05	0.0034	1.47E-04
Clougherty/Fenter	air	0.01	0.01	1173	7.52E-05	0.0144	3.49E-05
Berkowitz-Mattuck	37.5T O2-He	0.031	0.003	1173	7.10E-05	0.0044	1.08E-04

First, we show the model prediction across the entire temperature regime to illustrate the temperatures of transition and how the transition affects several parameters. Fig. 4 shows the predictions for zirconia scale thickness, diboride recession, the external boria thickness and internal boria thickness in a single plot, as a function of temperature from 773K to 2500K. The predictions are for the conditions used by Tripp and Graham, i.e., 0.033 MPa of pure oxygen, and for a duration of 1 hour. At temperatures below 800K external boria forms, but above 800K, the flow of glassy boria is found to be important. The model predicts that this external boria thickness decreases with increasing temperature and is non-existent above 1273K. Above this temperature, the boria starts to recede inwards and is all gone at around 2073 K. Thus the intermediate temperature regime is predicted to be between 1273K and 2073K. Note that the recession and zirconia scale thicknesses are not affected significantly by the external boria layer formation, (<800K). Obviously, oxygen permeation through the porous channel is more difficult than through the continuous external layer. Above 2098K, there is a brief regime where ZrO_2 evaporation is negligible, but above 2400K, it is significant and accompanied by rapid acceleration of recession.

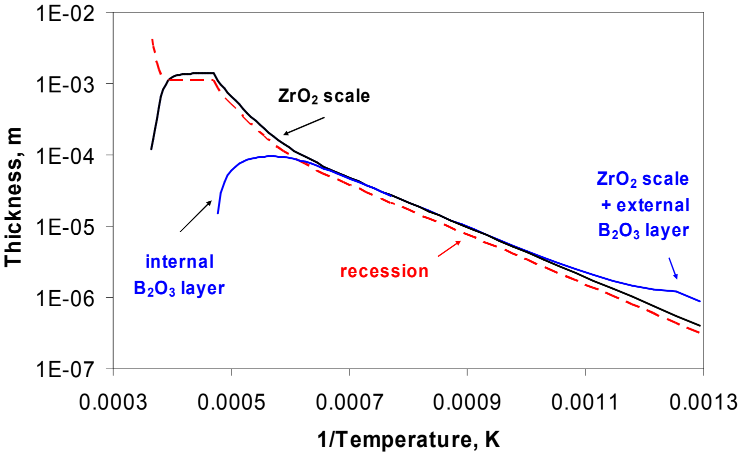

Fig. 4. Model predictions for zirconia scale thickness, diboride recession, the external boria thickness and internal boria thickness are shown as a function of temperature from 833K to 2500K. The predictions are for an exposure time of 1 hour in 0.033 MPa of pure oxygen.

Fig. 5 (a) shows the model predictions compared with the data of Tripp and Graham[8] for isothermal weight-gain versus time obtained in the low and intermediate temperature regimes. Fig. 5(b) shows the parabolic rate constants measured by Tripp and Graham[8, 25] at 0.033 MPa of oxygen, and the rate constants reported by Kuriakose and Margrave[25] at 0.099 MPa of oxygen.

There is reasonable agreement between the data and model predictions. Fig. 6 shows a comparison of model with reported measurements of recession by Clougherty and Fenter [6, 7] in air, and by Berkowitz-Mattuck[5] in 0.005 MPa O_2-He gas. Good correspondence is seen except for the temperature at which the recession accelerates in the high temperature regime. The rate of evaporation of zirconia is predicted to accelerate only above 2450K, while acceleration is seen at around 2050K. Spallation of the scale is one possible explanation for this discrepancy.

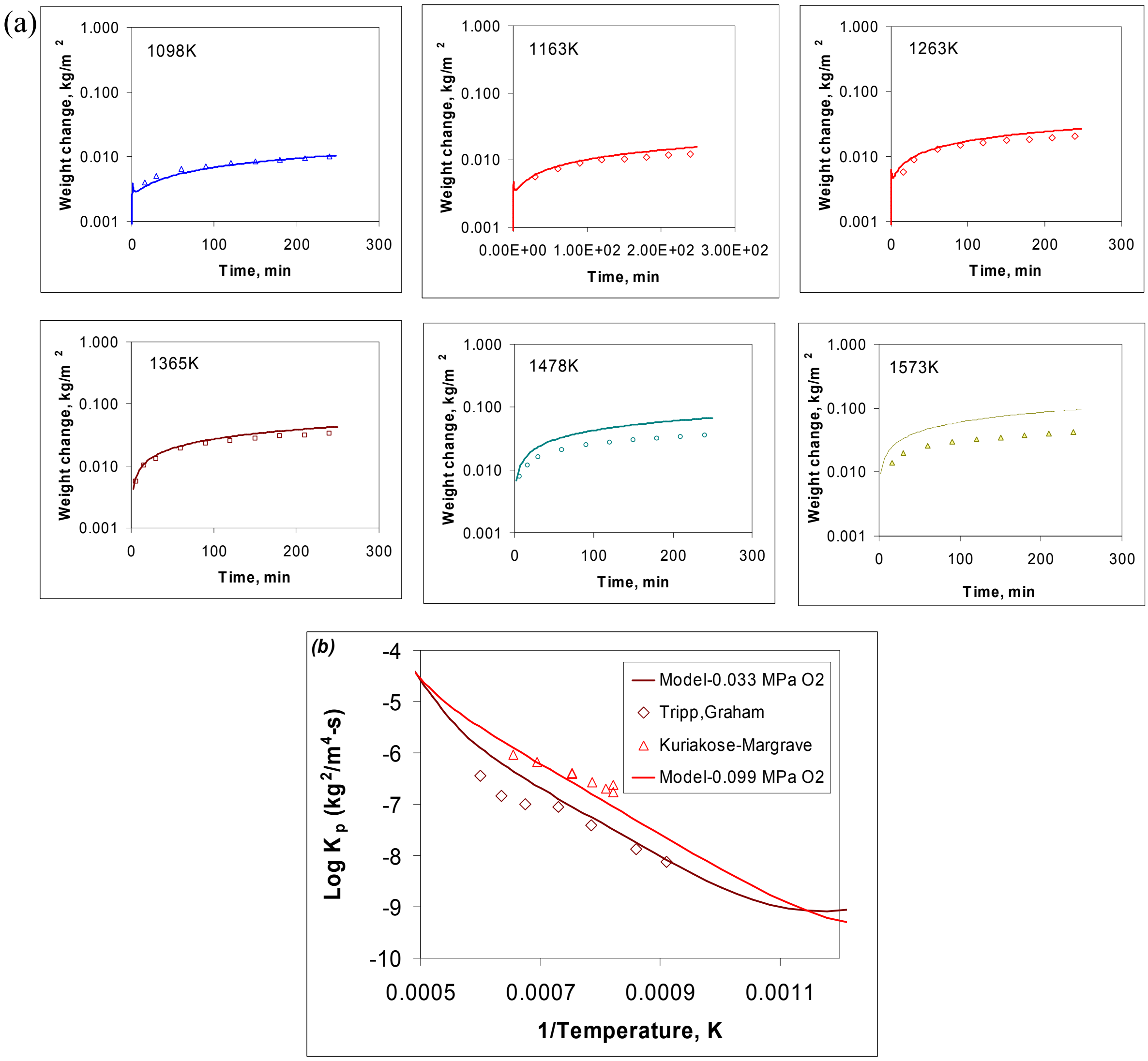

Fig. 5. Comparison of model predictions with experimental data on (a) isothermal weight gain taken from Tripp and Graham [8] (b) parabolic rate constants, taken from Tripp and Graham [8], Kuriakose and Margrave[25] (model shown as lines, and data as points)

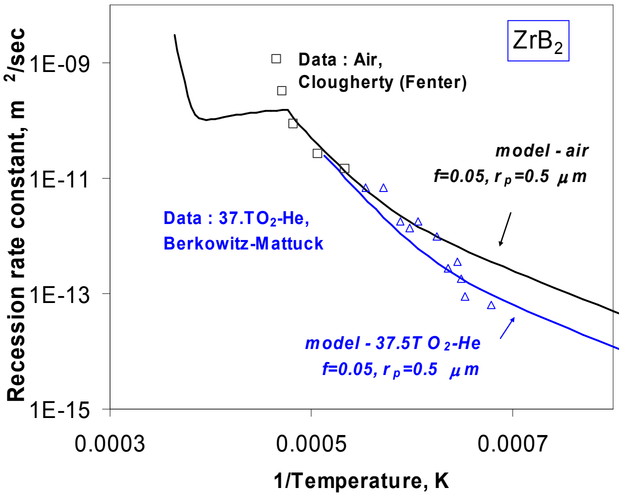

Fig. 6. Comparison of model predictions with experimental data on recession of diboride. The high-temperature data in air (1h) are from Fenter [7], and the intermediate temperature data in 0.005 MPa O_2-He are from Berkowitz-Mattuck.[5] (model shown as lines, data as points)

Summary

The transition in oxidation mechanisms of diborides was modeled as a function of temperature. The model assumed that at all temperatures a porous zirconia forms. At lower temperatures there is an external layer of boria, but its thickness can decrease due to either viscous flow or evaporation. In the intermediate temperature regime, the boria recedes within the pores of zirconia. At the high temperature regime, the zirconia is dry and can evaporate as gaseous zirconia. This model was evaluated using data on ZrB_2 measured under different experimental conditions. The agreement with experiments is found to be very reasonable for most conditions in the low and intermediate temperature regimes. The temperature at which zirconia vaporization accelerates recession in the high temperature regime is overpredicted by several hundred degrees. The possibility of scale spallation was ignored in the model, but may have been present under the experimental conditions.

Acknowledgments

We acknowledge useful discussions with Dr. I. Talmy of NSWC, MD, and Dr. Joan Fuller of the US Air Force Office of Scientific Research (AFOSR). This work was supported in part by USAF Contract # FA8650-04-D-5233.

References

---

[1] L. Kaufman, E. Clougherty, Technical Report RTD-TDR-63-4096 : Part 1, AFML, WPAFB, OH (1963).

[2] L. Kaufman, E. Clougherty, Technical Report RTD-TDR-63-4096 : Part 2, AFML, WPAFB, OH (1965).

[3] S. R. Levine, E. J. Opila, M. C. Halbig, J. D. Kiser, M. Singh, J. A. Salem, Jl Eur. Ceram. Soc. 22 (2002) 2757-2767.

[4] E. Opilla, S. Levine, J. Lorincz, Jl of Mater. Sci. 39 (2004) 5969-5977.

[5] J. B. Berkowitz-Mattuck, J. Electrochem. Soc. 113 (1966) 908.

[6] E. V. Clougherty, R. L. Pober, L. Kaufman, Trans. Met. Soc. AIME 242 (1968) 1077-1082.

[7] J. R. Fenter, SAMPE Quarterly 2,3 (1971).

[8] W. C. Tripp, H. C. Graham, J. Electrochem. Soc. 118 (1971) 1195-1199.

[9] L. Scatteia, R. Borrelli, G. Marino, A. Bellosi, F. Monteverde, Characterization and process of new metal diboride compound for TPS applications, in: AIAA/CIRA 13th Int. Space planes and hyperosnics systems and technologies, AIAA, 2005, p. 3267.

[10] F. Monteverde, Corrosion science 47 (2005) 2020-2033.

[11] F. Monteverde, A. Bellosi, J Electrochem.Soc. 150 (2003) B552-559.

[12] R. Savino, M. D. S. Fumo, D. Paterna, M. Serpico, Aerospace Sci and Tech. 9 (2005) 151-160.

[13] D. J. Thomas, NASA tech reoprt, NASA/CR-2002-211505 (2002).

[14] M. M. Opeka, I. G. Talmy, E. J. Wuchina, J. A. Zaykoski, S. J. Causey, Jl. Eur. Ceram. Soc. 19 (1999) 2405-2414.

[15] M. M. Opeka, I. G. Talmy, J. A. Zaykoski, J. Mater. Sci. 39 (2004) 5887-5904.

[16] E. Wuchina, M. Opeka, S. Causey, K. Buesking, J. Spain, A. Cull, J. Routbort, F. Guitierrez-Mora, J. Mater. Sci. 39 (2004) 5939-5949.

[17] I. Talmy, J. Zaykoski, M. Opeka, A. Smith, Personal communication of unpublished work (2005).

[18] W. G. Fahrenholtz, J. Amer. Ceram. Soc. 88 (2005) 3509-3512.

[19] T. A. Parthasarathy, R. A. Rapp, M. Opeka, R. J. Kerans, Acta Mater. 55 (2007) 5999-6010.

[20] T. Tokuda, T. Ido, T. Yamaguchi, Z Natuforschung 26A (1971) 2058-2060.

[21] R. H. Perry, C. H. Chilton, Chemical Engineers' Handbook, McGraw-Hill Book Company, 1973.

[22] P.-C. Li, A. C. Ghose, G.-J. Su, J Amer Ceram.Soc. 45 (1962) 83-88.

[23] H. C. Graham, H. H. Davis, J Amer Ceram.Soc. 54 (1971) 89-93.

[24] I. Barin, Thermochemical Data of Pure Substances I, VCH Verlagsgesellschaft:, New York, 1995.

[25] A. K. Kuriakose, J. L. Margrave, J. Electrochem. Soc. 111 (1964) 827.